A Framework for Discrete-Time $\mathcal{H}_2$ Preview Control

A. J. Hazell
e-mail: a.hazell@imperial.ac.uk

D. J. N. Limebeer[1]
e-mail: d.limebeer@imperial.ac.uk

Department of Electrical and Electronic Engineering,
Imperial College London,
London SW7 2AZ, UK

The purpose of this paper is to provide a set of synthesis and design tools for a wide class of $\mathcal{H}_2$ preview control systems. A generic preview design problem, which features both previewable and nonpreviewable disturbances, is embedded in a standard generalized regulator framework. Preview regulation is accomplished by a two-degrees-of-freedom output-feedback controller. A number of theoretical issues are studied, including the efficient solution of the standard $\mathcal{H}_2$ full-information Riccati equation and the efficient evaluation of the full-information preview gain matrices. The full-information problem is then extended to include the efficient implementation of the output-feedback controller. The synthesis of feedforward controllers with preview is analyzed as a special case—this problem is of interest to designers who wish to introduce preview as a separate part of a system design. The way in which preview reduces the $\mathcal{H}_2$-norm of the closed-loop system is analyzed in detail. Closed-loop norm reduction formulas provide a systematic way of establishing how much preview is required to solve a particular problem, and determine when extending the preview horizon will not produce worthwhile benefits. The paper concludes with a summary of the main features of preview control, as well as some controller design insights. New application examples are introduced by reference.
[DOI: 10.1115/1.4000810]

1 Introduction

There are many situations in which reference signals or future disturbances are "previewable." Optimal preview control is concerned with designing controllers that exploit previewed information in order to achieve performance levels that are superior to those achievable using current information alone. This paper considers the generic preview synthesis problem illustrated in Fig. 1, which comprises a two-degrees-of-freedom controller and both previewed disturbances/references (r) and unpreviewed disturbances (w). An $\mathcal{H}_2$-optimal solution to this controller synthesis problem is provided that requires only low-dimensional computations and low-dimensional Riccati equation solutions, and leads to a controller whose high-dimensional component is a finite impulse response (FIR) filter; the efficient implementation of FIR filters is well known in the signal processing literature. The low-dimensional solution to the problem described in Fig. 1 derives from the fact that the states of the (high-dimensional) delay line can be reconstructed by making a copy of Φ in the controller. The objective of this paper is to provide a framework for synthesizing preview controllers for any problem that fits into the framework illustrated in Fig. 1. In addition, we aim to provide some general insights into the design of preview controllers and a method for assessing the effectiveness of preview in terms of the achievable $\mathcal{H}_2$-norm reduction.

One of the first papers to recognize the importance of preview control is Ref. [1], in which three preview control models are described. In the third of these models, open-loop optimal preview controls are found using dynamic programming. The earliest applied work on preview control dates back to that in Ref. [2], where the Wiener filter theory was used to design an active suspension with road preview. This solution was not implementable, as it required the transfer function from the previewed path to the vehicle's acceleration to be unstable. Much of the subsequent work on preview tracking has its origins from the thesis done by Tomizuka [3], in which the preview control task is cast in a discrete-time linear quadratic regulator framework by augmenting the plant dynamics with a delay line model. In this formulation, the number of states grows in direct proportion to the preview length and so a direct solution of the corresponding Riccati equations becomes computationally infeasible for long preview lengths. Tomizuka [3] presented an efficient recursive method for solving these large equations. A continuous-time version of a LQ preview control problem is studied in Ref. [4], while a continuous-time preview control problem is given a stochastic interpretation in Ref. [5].

In the context of the early literature, Ref. [6] provides a good overview of an output-feedback preview-tracking problem with reference noise. This paper also summarizes many of the basic properties of preview feedback controllers. Motivated by a process control problem, another previewable command reference variant, the so-called proportional, integral, derivative, preview (PIDP) controller is studied in Ref. [7] in a LQ optimal control framework. A closely associated feedforward problem is studied in Ref. [8]. Other schemes for computing a feedforward-only controller is given in Refs. [9,10]. The vehicle suspension preview problem by Bender [2] is revisited in Ref. [11] in a discrete-time command preview framework. The preview suspension problem has attracted the attention of several practitioners in the more recent literature; examples include Refs. [12–15].

We will use the problem formulation in Fig. 1 as a basis for the results presented here. A solution will be derived by formulating the problem in a generalized regulator framework [16,17], and then finding efficient solutions to the resulting high-dimension Riccati equations. Contributions made by this paper include:

- an efficient method for finding the $\mathcal{H}_2$-norm of the closed-loop system
- a method for evaluating the benefit of preview
- a low-order output-feedback controller implementation
- an analysis of the generic properties of preview controllers

Figure 2 illustrates a simple example that may be used to highlight the benefit of preview, the broad structure of the controller, and the effect of preview on the achievable $\mathcal{H}_2$-norm of the closed-loop system. The preview action arises from the delay line Φ. The input to the controller is r, which is the future value of the

[1] Corresponding author.

Contributed by Dynamic Systems Division of ASME for publication in the Journal of Dynamic Systems, Measurement, and Control. Manuscript received August 22, 2007; final manuscript received June 18, 2009; published online xxxxx-xxxxx-xxxxx. Assoc. Editor: J. Karl Hedrick.

Incorrect symbols. The psfrag command has not been correctly used.

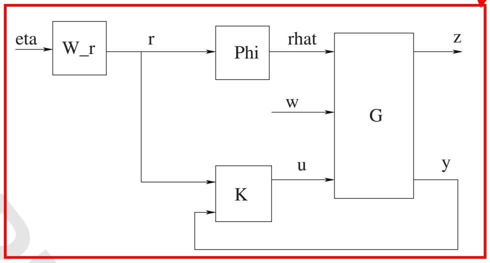

Fig. 1 A generalized regulator problem with both previewable and nonpreviewable disturbances. The transfer function G is the system to be controlled, K is the controller to be synthesized, and $\Phi = I\mathcal{Z}^{-N}$ is an N-step delay line (where $\mathcal{Z}$ is the Z-transform variable). The disturbance w is not previewable, the control and measurement signals are u and y, respectively, $\hat{r}$ is the previewable disturbance, and r is the future value of $\hat{r}$. The filter W_r is used to model the expected frequency content of r.

APC: #6

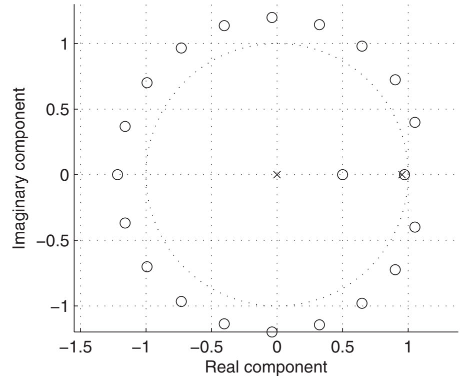

Fig. 3 Pole-zero plot of the $\mathcal{H}_2$-optimal $K(\mathcal{Z})$ for the case where $c_z=1.05$, $G(\mathcal{Z})=(\mathcal{Z}-c_z)/(\mathcal{Z}-0.5)$ and $N=20$. Crosses represent the poles and circles represent the zeros.

reference, and K is chosen so as to ensure that e is "small," and hence the plant output follows Φr as closely as possible. Define the error system

$$E(\mathcal{Z}) = G(\mathcal{Z})K(\mathcal{Z}) - \Phi(\mathcal{Z})$$

and assume that $G(\mathcal{Z})$ is stable; in the case that $G(\mathcal{Z})$ is unstable, it could be replaced by $\hat{G}(\mathcal{Z})=G(\mathcal{Z})(1-G(\mathcal{Z})K_f(\mathcal{Z}))^{-1}$ in which $K_f(\mathcal{Z})$ is a stabilizing feedback controller. Providing that $G(\mathcal{Z})$ has all its zeros inside the unit circle, perfect tracking ($E(\mathcal{Z})=0$) may be achieved by simply setting $K(\mathcal{Z})=G(\mathcal{Z})^{-1}\Phi(\mathcal{Z})$. However, if $G(\mathcal{Z})$ is a nonminimum phase (NMP), then such a $K(\mathcal{Z})$ is not internally stabilizing and a controller must be found that recognizes the limits imposed by NMP zeros on the achievable tracking performance.

For the case where $G(\mathcal{Z})$ is an arbitrary stable rational transfer function having a single real NMP zero at c_z, the $\mathcal{H}_2$-optimal controller is easily found. Our objective is to find an internally stabilizing $K(\mathcal{Z})$ such that $\|E(\mathcal{Z})\|_2$ is minimized.

The following inner-outer factorization may be performed:

$$G(\mathcal{Z}) = G_o(\mathcal{Z})G_i(\mathcal{Z})$$

where

$$G_i(\mathcal{Z}) = \frac{\mathcal{Z}-c_z}{1-\mathcal{Z}c_z}$$

We can write $E(\mathcal{Z})=(\tilde{K}(\mathcal{Z})-\Phi(\mathcal{Z})G_i(\mathcal{Z}^{-1}))G_i(\mathcal{Z})$ in which $\tilde{K}(\mathcal{Z}) = K(\mathcal{Z})G_o(\mathcal{Z})$ with $G_i(\mathcal{Z}^{-1})G_i(\mathcal{Z})=1$. The optimal controller is found by setting $K(\mathcal{Z})=(\Phi(\mathcal{Z})G_i(\mathcal{Z}^{-1}))_+G_o^{-1}(\mathcal{Z})$, where $(\cdot)_+$ denotes the stable projection [18,16]. It follows by direct calculation that:

Incorrect symbols. The psfrag command has not been correctly used.

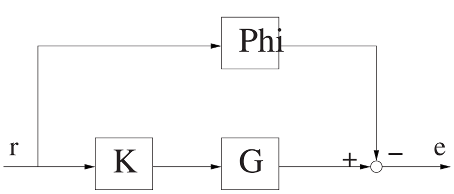

Fig. 2 A simple SISO open-loop preview-tracking problem. The transfer function $\Phi=\mathcal{Z}^{-N}$ is an N-step delay, G is the plant to be controlled, and K is a feedforward controller. The signal r is the *future* value of the reference, and e is the tracking error.

$$K(\mathcal{Z}) = \underbrace{G_o(\mathcal{Z})^{-1}}_{\text{IIR}}\underbrace{\left(-c_z^{-1}\mathcal{Z}^{-N} + (1-c_z^{-2})c_z\sum_{i=1}^{N}(\mathcal{Z}^{i-N}/c_z^i)\right)}_{\text{FIR}}$$

and that

$$\|E(\mathcal{Z})\|_2 = \frac{1}{|c_z^{N+1}|}\sqrt{c_z^2-1} \qquad (1)$$

Since $\|E(\mathcal{Z})\|_2 \to 0$ as $N\to\infty$, we conclude that in this example, preview action can overcome completely the tracking limitation imposed by the NMP zero. The optimal controller contains a high-order FIR part and a low-order infinite impulse response (IIR) part, where the preview action comes from the FIR part. The dynamics of the FIR block is fully specified by the RHP zero c_z and the preview length N. The fact that the high-order part of the controller is a FIR leads to an efficient hardware implementation.

A pole-zero plot of the optimal controller is given in Fig. 3 for the case where $c_z=1.05$, $G_o(\mathcal{Z})=(1-\mathcal{Z}c_z)/(\mathcal{Z}-0.5)$, and $N=20$. Notice the almost pole-zero cancellation on the real axis. In the limit $N\to\infty$, cancellation occurs. This simple preview problem highlights several important features that will be carried over into the more complex problem treated in this paper. In particular:

(1) The preview action is captured in a FIR block having order N.
(2) The remainder of the controller (the IIR part) has order equal to the plant order.
(3) The preview length (N) required to achieve 95% (for example) of the maximum norm reduction due to preview, is affected by the position of NMP zeros.

Point 3 merits further discussion. A central tenet of this paper is that the preview length could be sufficiently large that solution of the associated discrete algebraic Riccati equation (DARE) is computationally intractable. However, it might be argued that it is never necessary to use a large preview length because one could simply reduce the sampling rate until N becomes sufficiently small. In Ref. [19], an example similar to Fig. 2 is treated in continuous-time, and it is found that the required preview *time* is purely a function of the position of the continuous-time zero. The discrete-time equivalent of this result is: for a given performance improvement, the preview time NT_s (where T_s represents the sample time) is determined by the position of the continuous-time zero. This fact can be seen by considering the effect of T_s on the magnitude of c_z in Ref. [1]. Typically, the sampling rate is determined by the frequency at which tracking or disturbance rejection is required, and also by the frequency of any unstable poles [20]. It therefore follows that a combination of low-frequency zeros (which impose a large NT_s) and higher frequency performance specifications or unstable poles (which impose a low T_s) would lead unavoidably to a large preview length (N).

At this stage, the reader might be left with the impression that preview is of no benefit for minimum phase (MP) systems. However, as an example, it can be shown that the minimum achievable $\mathcal{H}_2$-norm of the transfer function

$$\begin{bmatrix} E(\mathcal{Z}) \\ \rho K(\mathcal{Z}) \end{bmatrix}$$

is reduced by preview action, even when $G(\mathcal{Z})$ is MP. By adding the additional term $\rho K(\mathcal{Z})$ into the optimization, we are effectively penalizing the magnitude of the control action. In general, a large ρ leads to a slow response and so a large N is required in order to get the full benefit from preview action. A detailed analysis of the effects of preview on systems of this form is given in Ref. [21] (~~see Ref. [21]~~, chapter 4).

The paper is structured as follows: Preliminaries and some standard notation is given in Sec. 2. A state-space description of the generalized regulator problem with both previewable and nonpreviewed exogenous disturbances is derived in Sec. 3. The solution of this problem, which is illustrated in Fig. 1, is the central focus of the paper. Following a summary of the general theory, the full-information preview control problem is solved in Sec. 4. The results are mainly concerned with efficient algorithms for solving the $\mathcal{H}_2$ full-information Riccati equation, and the evaluation of the full-information feedback gain matrix. The solution of the output-feedback preview problem is given in Sec. 5. The output-feedback controller involves a combination of a state estimator, and the solution to the full-information problem. An efficient controller synthesis is also given in this section. The effect of preview in reducing the $\mathcal{H}_2$-norm of the closed-loop system is analyzed in Sec. 6. The special case of feedforward control with preview is analyzed in Sec. 7. A summary of the main features of preview controllers, as well as some design insights, are given in Sec. 8. The conclusions are given in Sec. 9.

2 Notation and Preliminaries

We will make use of discrete-time state-space models of the form

$$\boldsymbol{x}(k+1) = \boldsymbol{A}\boldsymbol{x}(k) + \boldsymbol{B}\boldsymbol{u}(k)$$

$$\boldsymbol{y}(k) = \boldsymbol{C}\boldsymbol{x}(k) + \boldsymbol{D}\boldsymbol{u}(k)$$

in which k is the time index; $\boldsymbol{x}(k)$ is a vector of state variables; $\boldsymbol{u}(k)$ is a vector of inputs; $\boldsymbol{y}(k)$ is a vector of outputs; and $\boldsymbol{A}$, $\boldsymbol{B}$, $\boldsymbol{C}$, and $\boldsymbol{D}$ are appropriately dimensioned real matrices. Signals will sometimes be represented by omitting the time index, e.g.,

$$\boldsymbol{x} = \{\boldsymbol{x}(k)\}_{-\infty}^{\infty}$$

When transfer functions are associated with these models, they are computed using

$$G(\mathcal{Z}) = \boldsymbol{C}(\mathcal{Z}I - \boldsymbol{A})^{-1}\boldsymbol{B} + \boldsymbol{D}$$

in which $\mathcal{Z}$ is the Z-transform variable. We will also use the shorthand notation

$$G(\mathcal{Z}) \stackrel{s}{=} \left[\begin{array}{c|c} \boldsymbol{A} & \boldsymbol{B} \\ \hline \boldsymbol{C} & \boldsymbol{D} \end{array}\right] \tag{2}$$

The transfer function $G(\mathcal{Z})$ will be abbreviated by G when no confusion will occur.

The (lower) linear fractional transformation of the transfer-function matrices

$$P = \begin{bmatrix} P_{11} & P_{12} \\ P_{21} & P_{22} \end{bmatrix}$$

and K will be written as $\boldsymbol{F}_l(P,K)$, where

$$\boldsymbol{F}_l(P,K) = P_{11} + P_{12}K(I - P_{22}K)^{-1}P_{21}$$

The trace of a matrix will be denoted $\mathrm{Tr}\{\boldsymbol{A}\}$.

The $\mathcal{H}_2$-norm of a transfer function $G(\mathcal{Z})$ will be denoted by $\|G(\mathcal{Z})\|_2$, and is defined by

$$\|G(\mathcal{Z})\|_2 = \frac{1}{2\pi}\int_{-\pi}^{\pi} \mathrm{Tr}\{G(e^{j\theta})' G(e^{j\theta})\} d\theta$$

If G has the realization (2), with $\boldsymbol{A}$ assumed stable, and $\boldsymbol{X}$ is a matrix, which satisfies

$$\boldsymbol{X} = \boldsymbol{A}'\boldsymbol{X}\boldsymbol{A} + \boldsymbol{C}'\boldsymbol{C}$$

then

$$\|G(\mathcal{Z})\|_2^2 = \mathrm{Tr}\{\boldsymbol{B}'\boldsymbol{X}\boldsymbol{B} + \boldsymbol{D}'\boldsymbol{D}\} \tag{3}$$

A transfer function that maps signal a to signal b will be denoted $T_{a\to b}$.

An $m\times p$-dimensional zero matrix will be denoted as $0_{m\times p}$ and an n-dimensional identity matrix will be written as I_n. The shorthand $0_m = 0_{m\times m}$ will also be used.

The complex conjugate transpose of $\boldsymbol{A}$ will be denoted $\boldsymbol{A}'$ and n-dimensional real vectors are denoted $\mathbb{R}^n$.

3 Problem Formulation

The $\mathcal{H}_2$-optimal preview controller is defined to be the K that minimizes $\|T_{v\to z}\|_\infty$, where $v = [\eta' \;\; w']'$ with w, η, and z defined in Fig. 1. In other words, we wish to choose K, which minimizes $\|\boldsymbol{F}_l(P,K)\|_2$, where P is the mapping

$$\begin{bmatrix} z \\ y \\ r \end{bmatrix} = \begin{bmatrix} P_{11} & P_{12} \\ P_{21} & P_{22} \end{bmatrix} \begin{bmatrix} \eta \\ w \\ u \end{bmatrix}$$

The signals satisfy: $w(k) \in \mathbb{R}^{l_w}$, $r(k) \in \mathbb{R}^{l_r}$, $\eta(k) \in \mathbb{R}^{l_r}$, $v(k) \in \mathbb{R}^{l}$ (i.e., $l = l_r + l_w$), $u(k) \in \mathbb{R}^m$, $y(k) \in \mathbb{R}^{q_g}$, and $z(k) \in \mathbb{R}^p$. Also, q is defined as $q = q_g + l_r$. The N-step delay line Φ has the realization

$$\Phi(\mathcal{Z}) = \mathcal{Z}^{-N} I_{l_r} \stackrel{s}{=} \left[\begin{array}{c|c} \boldsymbol{A}_p & \boldsymbol{B}_p \\ \hline \boldsymbol{C}_p & 0_{l_r\times l_r} \end{array}\right]$$

with $\boldsymbol{A}_p$, $\boldsymbol{B}_p$ and $\boldsymbol{C}_p$ defined by

$$\boldsymbol{A}_p = \begin{bmatrix} 0_{l_r} & I_{l_r} & \cdots & 0_{l_r} \\ \vdots & \vdots & & \vdots \\ 0_{l_r} & 0_{l_r} & \ldots & I_{l_r} \\ 0_{l_r} & 0_{l_r} & \ldots & 0_{l_r} \end{bmatrix}$$

and

$$\boldsymbol{B}_p = \begin{bmatrix} 0_{(N-1)l_r\times l_r} \\ I_{l_r} \end{bmatrix}, \quad \boldsymbol{C}_p = \begin{bmatrix} I_{l_r} & 0_{l_r\times(N-1)lr} \end{bmatrix}$$

where N represents the number of preview steps and $\boldsymbol{A}_p \in \mathbb{R}^{Nl_r\times Nl_r}$. Without loss of generality the square transfer function W_r is assumed to be outer [16,17], with realization

$$W_r \stackrel{s}{=} \left[\begin{array}{c|c} \boldsymbol{A}_r & \boldsymbol{B}_r \\ \hline \boldsymbol{C}_r & \boldsymbol{D}_r \end{array}\right]$$

where $\boldsymbol{A}_r \in \mathbb{R}^{n_r\times n_r}$. Also without loss of generality [16], the plant is assumed to have the realization

$$G \stackrel{s}{=} \left[\begin{array}{c|ccc} \boldsymbol{A}_g & \boldsymbol{B}_{1gr} & \boldsymbol{B}_{1gw} & \boldsymbol{B}_{2g} \\ \hline \boldsymbol{C}_{1g} & \boldsymbol{D}_{11gr} & \boldsymbol{D}_{11gw} & \boldsymbol{D}_{12} \\ \boldsymbol{C}_{2g} & \boldsymbol{D}_{21gr} & \boldsymbol{D}_{21gw} & 0 \end{array}\right]$$

where $\boldsymbol{A}_g \in \mathbb{R}^{n_g\times n_g}$.

The transfer function from η to $\left[\begin{smallmatrix} \hat{r} \\ r \end{smallmatrix}\right]$ has realization

$$\begin{bmatrix} A_d & B_d \\ [illegible] & \\ C_{d2} & D_r \end{bmatrix} = \begin{bmatrix} A_p & B_pC_r & B_pD_r \\ 0 & A_r & B_r \\ [illegible] & 0 & 0 \\ 0 & C_r & D_r \end{bmatrix}$$

font size too large

Incorrect alignment. Arrows should align with columns of matrix.

and so the generalized plant P has realization

's' should be immediately above equals sign

$$P \overset{s}{=} \begin{array}{c} \\ n_g \updownarrow \\ Nl_r+n_r \updownarrow \\ p \updownarrow \\ q \updownarrow \\ l_r \updownarrow \end{array} \begin{array}{c} \begin{array}{ccccc} \overset{n_g}{\leftrightarrow} & \overset{Nl_r+n_r}{\leftrightarrow} & \overset{l_r}{\leftrightarrow} & \overset{l_w}{\leftrightarrow} & \overset{m}{\leftrightarrow} \end{array} \\ \begin{bmatrix} A_g & B_{1gr}C_{d1} & 0 & B_{1gw} & B_{2g} \\ 0 & A_d & B_d & 0 & 0 \\ C_{1g} & D_{11gr}C_{d1} & 0 & D_{11gw} & D_{12} \\ C_{2g} & D_{21gr}C_{d1} & 0 & D_{21gw} & 0 \\ 0 & C_{d2} & D_r & 0 & 0 \end{bmatrix} \end{array} \tag{4}$$

$$\overset{s}{=} \begin{bmatrix} A & B_1 & B_2 \\ C_1 & D_{11} & D_{12} \\ C_2 & D_{21} & 0 \end{bmatrix} \tag{5}$$

The A-matrix in Eq. (5) satisfies $A \in \mathbb{R}^{n\times n}$ with $n = n_g + Nl_r + n_r$.

4 Full-Information Control Problem

4.1 Standard Theory. We begin with a brief summary of the discrete-time, linear time-invariant perfect information control problem [16], which has plant description

Incorrect alignment. Arrows should align with columns of matrix.

font size too large

$$P_{FI} \overset{s}{=} \begin{array}{c} \\ n \updownarrow \\ p \updownarrow \\ n \updownarrow \\ l \updownarrow \end{array} \begin{array}{c} \begin{array}{ccc} \overset{n}{\leftrightarrow} & \overset{l}{\leftrightarrow} & \overset{m}{\leftrightarrow} \end{array} \\ \begin{bmatrix} A & B_1 & B_2 \\ C_1 & D_{11} & D_{12} \\ I & 0 & 0 \\ 0 & I & 0 \end{bmatrix} \end{array}$$

and which satisfies the following standard assumptions:

no bullets required

- (A1) (A, B_2) is stabilizable.
- (A2) $D_{12}'D_{12} > 0$.
- (A3) $\mathrm{rank}\begin{bmatrix} A-e^{j\theta}I & B_2 \\ C_1 & D_{12} \end{bmatrix} = n+m, \quad \forall\, \theta \in (-\pi, \pi]$.

We would like to find the internally stabilizing controller K_{FI}, which minimizes $\|F_l(P_{FI}, K_{FI})\|_2$. First, define

$$\bar{R} = D_{12}'D_{12} + B_2'XB_2 \tag{6}$$

$$F_2 = -\bar{R}^{-1}(B_2'XA + D_{12}'C_1) \tag{7}$$

$$A_c = A + B_2F_2 \tag{8}$$

In Ref. [17] it is shown that if (A1)–(A3) are satisfied, then there exists a solution X to the DARE

$$X = A'XA - F_2'\bar{R}F_2 + C_1'C_1 \tag{9}$$

such that

$$X \geq 0 \tag{10}$$

$$A_c \text{ is asymptotically stable.} \tag{11}$$

A matrix X satisfying Eqs. (9) and (11) is said to be *stabilizing*. The internally stabilizing, full-information $\mathcal{H}_2$-optimal controller is then given by

$$K_{FI} = \begin{bmatrix} F_2 & F_0 \end{bmatrix} \tag{12}$$

with

$$F_0 = -\bar{R}^{-1}(B_2'XB_1 + D_{12}'D_{11})$$

The resulting closed-loop norm is given by

$$\|F_l(P_{FI}, K_{FI})\|_2^2 = \mathrm{Tr}\{(D_{11} + D_{12}F_0)'(D_{11} + D_{12}F_0) + (B_1 + B_2F_0)'X(B_1 + B_2F_0)\}$$

[illegible]ent Computation of the Full-Information [illegible] [illegible] this section, we will find an efficient solution for [illegible] Eq. (9) for the plant described in Sec. 3. First, we decompose Eq. (9) into an n_g-dimensional DARE, an Nl_r+n_r-dimensional discrete Lyapunov equation, and an $(n_g \times Nl_r+n_r)$-dimensional Stein equation. We then give an efficient solution to the Stein equation, and show how this leads to an efficient method for computing the full-information controller.

Lemma 4.1 (decomposition of the DARE). *Let X be the unique stabilizing and non-negative solution to the DARE in Eq. (9), and partition X as*

font size too large

$$X = \begin{array}{c} \\ n_g \updownarrow \\ Nl_r+n_r \updownarrow \end{array} \begin{array}{c} \begin{array}{cc} \overset{n_g}{\leftrightarrow} & \overset{Nl_r+n_r}{\leftrightarrow} \end{array} \\ \begin{bmatrix} X_{gg} & X_{gd} \\ X_{gd}' & X_{dd} \end{bmatrix} \end{array}$$

then X_{gg} is the unique stabilizing and non-negative solution to the DARE

$$X_{gg} = A_g'X_{gg}A_g - F_{2g}'\bar{R}F_{2g} + C_{1g}'C_{1g} \tag{13}$$

where

$$F_{2g} = -\bar{R}^{-1}(B_{2g}'X_{gg}A_g + D_{12}'C_{1g}) \tag{14}$$

in which $\bar{R}$ may be computed from

$$\bar{R} = B_{2g}'X_{gg}B_{2g} + D_{12}'D_{12} \tag{15}$$

Furthermore, X_{gd} and X_{dd} are the unique solutions to

$$X_{gd} = SC_{d1} + A_{cg}'X_{gd}A_d \tag{16}$$

$$X_{dd} = A_d'X_{dd}A_d + Q \tag{17}$$

with

$$S = A_g'X_{gg}B_{1gr} + F_{2g}'B_{2g}'X_{gg}B_{1gr} + F_{2g}'D_{12}'D_{11gr} + C_{1g}'D_{11gr}$$

$$A_{cg} = A_g + B_{2g}F_{2g}$$

$$F_{2d} = -\bar{R}^{-1}(B_{2g}'X_{gd}A_d + B_{2g}'X_{gg}B_{1gr}C_{d1} + D_{12}'D_{11gr}C_{d1})$$

$$Q = C_{d1}'B_{1gr}'X_{gg}B_{1gr}C_{d1} + A_d'X_{gd}'B_{1gr}C_{d1} + C_{d1}'B_{1gr}'X_{gd}A_d - F_{2d}'\bar{R}F_{2d} + C_{d1}'D_{11gr}'D_{11gr}C_{d1}$$

Proof. First, partition Eq. (7) conformably with X

$$F_2 = -\bar{R}^{-1}\left(\begin{bmatrix} B_{2g}' & 0 \end{bmatrix}\begin{bmatrix} X_{gg} & X_{gd} \\ X_{gd}' & X_{dd} \end{bmatrix}\begin{bmatrix} A_g & B_{1gr}C_{d1} \\ 0 & A_d \end{bmatrix} + D_{12}'\begin{bmatrix} C_{1g} & D_{11gr}C_{d1} \end{bmatrix}\right)$$

$$= -\bar{R}^{-1}\begin{bmatrix} B_{2g}'X_{gg}A_g + D_{12}'C_{1g} & B_{2g}'X_{gd}A_d + B_{2g}'X_{gg}B_{1gr}C_{d1} + D_{12}'D_{11gr}C_{d1} \end{bmatrix} = \begin{bmatrix} F_{2g} & F_{2d} \end{bmatrix} \tag{18}$$

and hence F_{2g} and F_{2d} form partitions of F_2. Now, partition Eq. (9) to obtain

$$\begin{bmatrix} X_{gg} & X_{gd} \\ X_{gd}' & X_{dd} \end{bmatrix} = \begin{bmatrix} A_g' & 0 \\ C_{d1}'B_{1gr}' & A_d' \end{bmatrix}\begin{bmatrix} X_{gg} & X_{gd} \\ X_{gd}' & X_{dd} \end{bmatrix}\begin{bmatrix} A_g & B_{1gr}C_{d1} \\ 0 & A_d \end{bmatrix} - \begin{bmatrix} F_{2g}' \\ F_{2d}' \end{bmatrix}\bar{R}\begin{bmatrix} F_{2g} & F_{2d} \end{bmatrix} + \begin{bmatrix} C_{1g}' \\ C_{d1}'D_{11gr}' \end{bmatrix} \times \begin{bmatrix} C_{1g} & D_{11gr}C_{d1} \end{bmatrix} \tag{19}$$

Equation (15) is easily checked, and so Eqs. (13), (16), and (17) follow immediately by considering, respectively, the top left, the top right, and the bottom right partitions of Eq. (19).

Now, note that

$$A_c = \begin{bmatrix} A_{cg} & \star \\ 0 & A_d \end{bmatrix}$$

in which A_d is stable. It now follows from assumption (A1) that X_{gg} is stabilizing if and only if X is stabilizing.

Note that F_{2g} and $\bar{R}$ are not functions of X_{gd} or X_{dd}, and so Eq. (13) may be solved independently by Eqs. (16) and (17). Since Eq. (16) depends on the solution of Eq. (13), it can be solved next. Finally, Eq. (17) depends on both Eqs. (13) and (16) and so it is necessarily solved last. The following result provides a fast algorithm for solving Eq. (16).

Lemma 4.2 (efficient solution of the Stein equation). *Consider the discrete Stein equation*

$$X_{gd} = SC_{d1} + A'_{cg} X_{gd} A_d \tag{20}$$

with A_{cg} stable. Partitioning $X_{gd}=[X_{gp}\ \ X_{gr}]$ compatibly with

$$A_d = \begin{bmatrix} A_p & B_p C_r \\ 0 & A_r \end{bmatrix}$$

gives

$$X_{gp} = \begin{bmatrix} S & A'_{cg}S & {A'_{cg}}^2 S & \ldots & {A'_{cg}}^{N-1} S \end{bmatrix} \tag{21}$$

$$X_{gr} = {A'_{cg}}^N S C_r + A'_{cg} X_{gr} A_r \tag{22}$$

Proof. Partitioning Eq. (20) leads to

$$X_{gp} = SC_p + A'_{cg} X_{gp} A_p \tag{23}$$

$$X_{gr} = A'_{cg} X_{gp} B_p C_r + A'_{cg} X_{gr} A_r \tag{24}$$

If we substitute Eq. (23) into itself M times we obtain

$$X_{gp} = {A'_{cg}}^{M+1} X_{gp} A_p^{M+1} + \sum_{k=0}^{M} {A'_{cg}}^k S C_p A_p^k$$

Since A_{cg} and A_p are stable, we may allow $M \to \infty$ and hence write

$$X_{gp} = \sum_{k=0}^{\infty} {A'_{cg}}^k S C_p A_p^k$$

However, since $A_p^N=0$ we may truncate the infinite sum to give

$$X_{gp} = \sum_{k=0}^{N-1} {A'_{cg}}^k S C_p A_p^k \tag{25}$$

The effect of postmultiplying by A_p^k is to shift the columns of the preceding matrix right by kl_r, and so $C_p A_p^k = [0_{l_r \times kl_r}\ \ I_{l_r}\ \ 0_{l_r \times (N-1-k)l_r}]$. Substituting this into Eq. (25) leads to Eq. (21). Now, substituting Eq. (21) into Eq. (24) leads to Eq. (22).

The following is obtained by substituting Eqs. (21) and (22) into the definitions for the controller gains F_2 and F_0.

Corollary 4.3 (efficient computation of full-information controller gains). *The matrix F_2 may be partitioned (compatibly with A) as $F_2=[F_{2g}\ \ F_{2p}\ \ F_{2r}]$ in which F_{2g} is given by* Eq. (14), *and*

$$\begin{aligned} F_{2p} = -\bar{R}^{-1}\big[& B'_{2g} X_{gg} B_{1gr} \\ & + D'_{12} D_{11gr} \quad B'_{2g} S \quad B'_{2g} A'_{cg} S \quad \ldots \quad B'_{2g} {A'_{cg}}^{N-2} S \big] \end{aligned} \tag{26}$$

$$F_{2r} = -\bar{R}^{-1}(B'_{2g} {A'_{cg}}^{N-1} S C_r + B'_{2g} X_{gr} A_r) \tag{27}$$

If we partition $F_0=[F_{0r}\ \ F_{0w}]$, then

$$F_{0r} = -\bar{R}^{-1}(B'_{2g} X_{gr} B_r + B'_{2g} A_{cg}^{N-1} S D_r) \tag{28}$$

$$F_{0w} = -\bar{R}^{-1}(B'_{2g} X_{gg} B_{1gw} + D'_{12} D_{11gw}) \tag{29}$$

Corollary 4.4. *As $N \to \infty$ the control becomes independent of the choice of W_r.*

Proof. Since A_r and A_{cg} are asymptotically stable, it follows from standard results that Eq. (22) has a unique solution. In the limit as $N \to \infty$, Eq. (22) implies that $X_{gr}=A'_{cg} X_{gr} A_r$ and so in the limit $X_{gr}=0$. Direct substitution into Eqs. (27) and (28), while taking the limit as $N \to \infty$, leads to

$$F_{2r} = 0 \quad \text{and} \quad F_{0r} = 0, \qquad \forall\, A_r, B_r, C_r, D_r$$

and so the control signal is independent of W_r.

Remark 4.5. If x_g and x_r are the states of G and W_r, respectively, then the optimal control is given by

$$u(k)^* = \underbrace{F_{2g} x_g(k)}_{\text{Feedback}} \underbrace{+ F_{2r} x_r(k) + F_{0r} \eta(k) + F_{0w} w(k) + \sum_{j=0}^{N-1} F_{2p,j} r(k-N+j)}_{\text{Feedforward}}$$

with

$$F_{2p,0} = -\bar{R}^{-1}(B'_{2g} X_{gg} B_{1gr} + D'_{12} D_{11gr})$$

$$F_{2p,j} = -\bar{R}^{-1} B'_{2g} A_{cg}^{j-1} S, \quad 1 \le j \le N-1$$

Remark 4.6. The feedback gain F_{2g} is precisely that which would be obtained if one were to search for a full-information controller that minimized $\|T_{w \to z}\|$, with W_r and Φ removed from the problem description. The choice of feedback control is therefore independent of the preview length.

Remark 4.7. The full-information controller that minimizes $\|T_{v \to z}\|_2$ also minimizes $\|T_{\eta \to z}\|_2$ and $\|T_{w \to z}\|_2$. This type of relationship is true for any partition of the exogenous disturbance signal in an $\mathcal{H}_2$ full-information generalized regulator problem, and it is not a particular feature of the preview control problem. To see this, note that the two minimization problems

$$\min_{K_{FI}} \|T_{\eta \to z}\|_2 \tag{30}$$

$$\min_{K_{FI}} \|T_{w \to z}\|_2 \tag{31}$$

are related by the choice of B_1 and D_{11}, and that computation of the controller gain F_2 is independent of these matrices. The feedforward control gains F_{0r} and F_{0w} can be chosen independently, and so it is possible to simultaneously minimize $\|T_{\eta \to z}\|_2$ and $\|T_{w \to z}\|_2$. Since $\|T_{v \to z}\|_2^2 = \|T_{\eta \to z}\|_2^2 + \|T_{w \to z}\|_2^2$, a controller satisfying Eqs. (30) and (31) also minimizes $\|T_{v \to z}\|_2$.

5 Output-Feedback Solution

5.1 Standard Theory. We now consider a discrete-time, linear, time-invariant system P of the form

$$P \overset{s}{=} \begin{array}{c c} & \begin{array}{ccc} \overset{n}{\leftrightarrow} & \overset{l}{\leftrightarrow} & \overset{m}{\leftrightarrow} \end{array} \\ \begin{array}{c} n\updownarrow \\ p\updownarrow \\ q\updownarrow \end{array} & \begin{bmatrix} A & B_1 & B_2 \\ C_1 & D_{11} & D_{12} \\ C_2 & D_{21} & 0 \end{bmatrix} \end{array}$$

See previous comments

which satisfies (A1)–(A3) as well as

- (A4) (A, C_2) is detectable.
- (A5) $D_{21} D'_{21} > 0$.
- (A6) $\operatorname{rank}\begin{bmatrix} A - e^{j\theta} I & B_1 \\ C_2 & D_{21} \end{bmatrix} = n + q, \quad \forall\, \theta \in (-\pi, \pi]$.

We wish to compute an internally stabilizing K that minimizes $\|F_l(P,K)\|_2$. Define

$$\bar{S} = D_{21}D_{21}' + C_2YC_2', \quad L_2 = -(AYC_2' + B_1D_{21}')\bar{S}^{-1}$$

If (A4)–(A6) are satisfied, it is shown in Ref. [17] that there exists a Y that solves

$$Y = AYA' - L_2\bar{S}L_2' + B_1B_1' \tag{32}$$

such that

$$Y \geq 0$$

$$A + L_2C_2 \text{ is asymptotically stable.}$$

If we define

$$L_0 = (F_2YC_2' + F_0D_{21}')\bar{S}^{-1}$$

then, according to Ref. [17], the $\mathcal{H}_2$-optimal output-feedback controller is given by

's' positioned incorrectly

$$K \overset{s}{=} \begin{bmatrix} A_K & B_K \\ C_K & D_K \end{bmatrix} \tag{33}$$

$$A_K = A + B_2F_2 + L_2C_2 - B_2L_0C_2 \tag{34}$$

$$B_K = -(L_2 - B_2L_0) \tag{35}$$

$$C_K = F_2 - L_0C_2 \tag{36}$$

$$D_K = L_0 \tag{37}$$

The $\mathcal{H}_2$-norm of the resulting closed-loop system is given by

$$\|F_l(P,K)\|_2^2 = \|F_l(P_{FI},K_{FI})\|_2^2 + \mathrm{Tr}\{\bar{R}((L_0D_{21} - F_0)(L_0D_{21} - F_0)' + (L_0C_2 - F_2)Y(L_0C_2 - F_2)')\}$$

5.2 Efficient Computation of Output-Feedback Controller. In this section we aim to find a computationally efficient solution to the DARE in Eq. (32), given that P has the structure described in Eq. (4). The results of this section do not depend on the internal structure of A_p, B_p, and C_p (though we do require that A_p is stable).

Lemma 5.1. *The stabilizing non-negative solution to* Eq. (32) *may be computed using*

see previous comments

$$Y = \begin{array}{c c} & \begin{array}{cc} \overset{n_g}{\leftrightarrow} & \overset{Nl_r+n_r}{\leftrightarrow} \end{array} \\ \begin{array}{r} n_g\updownarrow \\ Nl_r+n_r\updownarrow \end{array} & \begin{bmatrix} Y_g & 0 \\ 0 & 0 \end{bmatrix} \end{array}$$

where Y_g is the unique stabilizing and non-negative solution to

$$Y_g = A_gY_gA_g' - L_{2g}\bar{S}_gL_{2g}' + B_{1gw}'B_{1gw} \tag{38}$$

with

$$\bar{S}_g = D_{21gw}D_{21gw}' + C_{2g}Y_gC_{2g}', \quad L_{2g} = -(A_gY_gC_{2g}' + B_{1gw}D_{21gw}')\bar{S}_g^{-1}$$

Proof. Note that (A4)–(A6) imply

- (A4g) (A_g, C_{2g}) is detectable.
- (A5g) $D_{21gw}D_{21gw}' > 0$.
- (A6g) $\mathrm{rank}\begin{bmatrix} A_g - e^{j\theta}I & B_{1gw} \\ C_{2g} & D_{21gw} \end{bmatrix} = n_g + q_g, \quad \forall\, \theta \in (-\pi, \pi]$.

It then follows that (A4)–(A6) ensure the existence of a stabilizing non-negative solution to Eq. (38). Let Y_g be a stabilizing and non-negative solution to Eq. (38). We will now show that $Y = \left[\begin{smallmatrix} Y_g & 0 \\ 0 & 0 \end{smallmatrix}\right]$ is a stabilizing non-negative solution to Eq. (32).

It easily checked that the following hold, if $Y = \left[\begin{smallmatrix} Y_g & 0 \\ 0 & 0 \end{smallmatrix}\right]$:

$$\bar{S} = \begin{bmatrix} \bar{S}_g & 0 \\ 0 & D_rD_r' \end{bmatrix}$$

$$L_2 = \begin{bmatrix} L_{2g} & 0 \\ 0 & -B_dD_r^{-1} \end{bmatrix}$$

$$B_1B_1' = \begin{bmatrix} B_{1gw}B_{1gw}' & 0 \\ 0 & B_dB_d' \end{bmatrix}$$

$$AYA' = \begin{bmatrix} A_gY_gA_g' & 0 \\ 0 & 0 \end{bmatrix} \tag{39}$$

where the invertibility of D_r is guaranteed by assumption (A5), together with the fact that W_r is square. It then follows that:

$$AYA' - L_2\bar{S}L_2' + B_1B_1' = \begin{bmatrix} A_gY_gA_g' - L_{2g}\bar{S}_g\bar{L}_{2g}' + B_{1gw}B_{1gw}' & 0 \\ 0 & 0 \end{bmatrix} = \begin{bmatrix} Y_g & 0 \\ 0 & 0 \end{bmatrix} = Y$$

Therefore, if Y_g solves Eq. (38), then $Y = \left[\begin{smallmatrix} Y_g & 0 \\ 0 & 0 \end{smallmatrix}\right]$ solves Eq. (32). We now need to check that Y is stabilizing. Note that

$$A + L_2C_2 = \begin{bmatrix} A_g + L_{2g}C_{2g} & \star \\ 0 & A_d - B_dD_r^{-1}C_{d2} \end{bmatrix}$$

The matrix $A_d - B_dD_r^{-1}C_{d2}$ is stable because

$$A_d - B_dD_r^{-1}C_{d2} = \begin{bmatrix} A_p & 0 \\ 0 & A_r - B_rD_r^{-1}C_r \end{bmatrix} \tag{40}$$

in which A_p is stable by definition and $A_r - B_rD_r^{-1}C_r$ is stable because W_r is assumed to be outer. Since Y_g is stabilizing, we know that $A_g + L_{2g}C_{2g}$ is stable, and hence that $A + L_2C_2$ is stable, as required.

psfrag not used

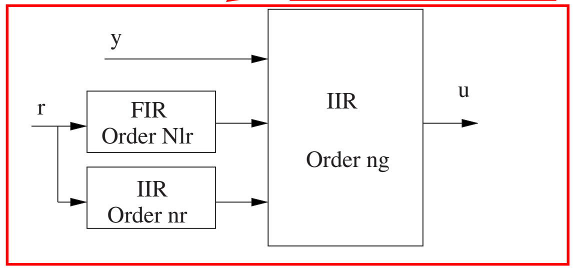

Fig. 4 Structure of the $\mathcal{H}_2$-optimal preview controller. The signal u is the control, the measurement is y, and r is the future value of the previewable disturbance. The preview length is N, l_r is the dimension of r, n_r is the order of W_r, and n_g is the order of G.

5.3 Efficient Implementation. We now have a complete method for efficiently computing the output-feedback preview controller; however, in its present form, this controller has the same order as the generalized plant. In general, a controller of this order cannot be implemented. Fortunately, the high-order part of the controller is a FIR filter (illustrated in Fig. 4) for which efficient implementations exist.

This controller structure is proven in the following lemma.

Lemma 5.2. *The optimal controller described in* Eq. (33) *for the plant in* Eq. (4) *can be written in the form*

$$K \overset{s}{=} \begin{bmatrix} A_K & B_K \\ C_K & D_K \end{bmatrix} = \begin{bmatrix} A_{Kgg} & A_{Kgp} & A_{Kgr} & B_{Kgy} & B_{Kgr} \\ 0 & A_p & 0 & 0 & B_p \\ 0 & 0 & A_r - B_rD_r^{-1}C_r & 0 & B_rD_r^{-1} \\ C_{Kg} & C_{Kp} & C_{Kr} & L_{0y} & F_{0r}D_r^{-1} \end{bmatrix} \tag{41}$$

where $A_{Kgg} \in \mathbb{R}^{n_g \times n_g}$ and $B_{Kgg} \in \mathbb{R}^{n_g \times l_w}$ and psfrag

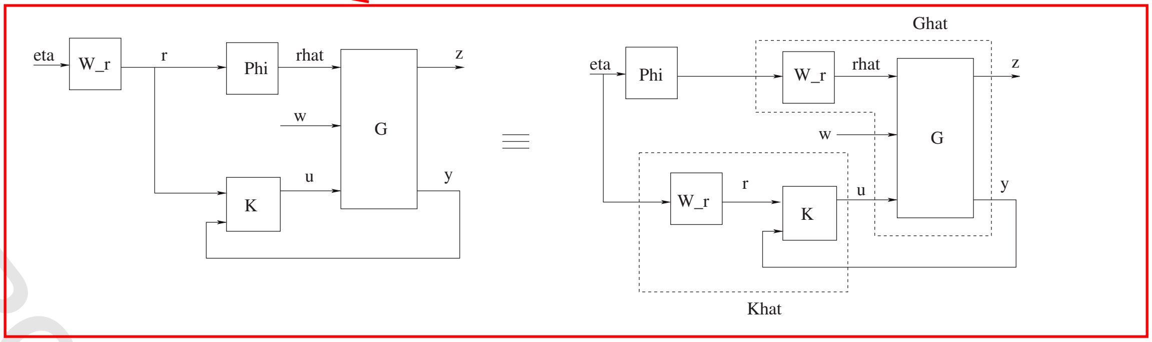

Fig. 5 Two equivalent representations of the previewable disturbance rejection problem. These representations are equivalent in the sense that the transfer functions from η and w to z and y are identical. Recall that $\Phi = \mathcal{Z}^{-N} I$, which commutes with W_r under multiplication.

$$L_{0y} = (F_{2g} Y_g C_{2g}' + F_{0w} D_{21gw}') \bar{S}_g^{-1}$$

$$A_{Kgg} = A_g + B_{2g} F_{2g} + L_{2g} C_{2g} - B_{2g} L_{0y} C_{2g}$$

$$A_{Kgp} = B_{1gr} C_p + B_{2g} F_{2p} + L_{2g} D_{21gr} C_p - B_{2g} L_{0y} D_{21gr} C_p$$

$$A_{Kgr} = B_{2g} F_{2r} - B_{2g} F_{0r} D_r^{-1} C_r$$

$$B_{Kgy} = -(L_{2g} - B_{2g} L_{0g})$$

$$B_{Kgr} = B_{2g} F_{0r} D_r^{-1}$$

$$C_{Kg} = F_{2g} - L_{0y} C_{2g}$$

$$C_{Kp} = F_{2p} - L_{0y} D_{21gr} C_p$$

$$C_{kr} = F_{2r} - F_{0r} D_r^{-1} C_r$$

Proof. The realization given in Eq. (41) follows from Eq. (33), together with Eqs. (39) and (40), and $L_0 = [L_{0y} \;\; F_{0r} D_r^{-1}]$.

This then leads to the low-order implementation

$$\bar{K} \overset{s}{=} \left[\begin{array}{c|cccc} A_{Kgg} & A_{Kgr} & B_{Kgy} & A_{Kgp} & B_{Kgr} \\ 0 & A_r - B_r D_r^{-1} C_r & 0 & 0 & B_r D_r^{-1} \\ \hline C_{Kg} & C_{Kr} & L_{0y} & C_{Kp} & F_{0r} D_r^{-1} \end{array}\right] \tag{42}$$

where the optimal control is given by

$$u^* = \bar{K} \begin{bmatrix} y \\ \bar{r} \end{bmatrix}$$

$$\bar{r}(k) = \begin{bmatrix} r(k-N) \\ \vdots \\ r(k) \end{bmatrix}$$

Corollary 5.3. *The output-feedback controller that minimizes $\|T_{v \to z}\|_2$, also minimizes $\|T_{\eta \to z}\|_2$ and $\|T_{w \to z}\|_2$.*

Proof. The controller may be decomposed into feedback and feedforward components K_{fb} and K_{ff}, so that

$$u^* = K_{fb} y + K_{ff} r$$

with K_{fb} given by

$$K_{fb} \overset{s}{=} \left[\begin{array}{c|c} A_{Kgg} & B_{Kgy} \\ \hline C_{Kg} & L_{0y} \end{array}\right]$$

The transfer function $T_{w \to z}$ is determined by K_{fb} and P, and it is easily checked that K_{fb} is precisely the controller, which is obtained by minimizing $\|T_{w \to z}\|_2$ alone.

It is well known that the $\mathcal{H}_2$-optimal controller has an observer structure. If $w = 0$, then the observer will contain an exact copy of the states of G and W_r (once initial transients have decayed). Therefore, the closed-loop transfer function $T_{r \to z}$ will be precisely the same as that resulting from the application of the full-information controller K_{FI} to the plant P_{FI}. Remark 4.7 implies that the value of $\|T_{r \to z}\|_2$ achieved by this controller is indeed minimal.

Unlike the full-information case, this result is not a general property of any partition of the exogenous disturbance signal, instead it results from the particular structure considered here. The result is useful because it leads us to the conclusion that the choice of W_r does not alter the resulting $T_{w \to z}$, and so W_r tunes only the response to the previewable signal.

6 Reduction in $\mathcal{H}_2$-Norm Due to Preview

The purpose of this section is to derive an efficient means of computing the minimum achievable closed-loop $\mathcal{H}_2$-norm for a given preview length. In so doing, we provide tools to answer the questions:

- What is the preview length required to achieve a given performance specification?
- What is the maximum possible reduction in the closed-loop $\mathcal{H}_2$-norm through preview?
- If a large amount of preview is available, how much should be used?

For the purposes of computing the minimum achievable $\mathcal{H}_2$-norm, we may assume $W_r = I$ without loss of generality. The transformation that enables us to make this assumption is illustrated in Fig. 5. The design problem involving $\hat{K}$ and $\hat{G}$ is clearly a problem of the class of Fig. 1, but without a prefilter. The achievable $\mathcal{H}_2$-norm will be the same in either case, and in this section we will work with the simpler problem setup, where it is assumed that W_r has been absorbed into $\hat{G}$ and $\hat{K}$. This transformation is not used in the preceding sections because it obscures the impact of W_r on the control signal, and because we would be required to perform further manipulations in order to remove the additional controller states resulting from the extra copy of W_r.

It is easy to check that the results of the previous sections carry over for $W_r = I$. All that is required is to remove the gains associated with the states of W_r.

We note again that

$$\|T_{[r' w']' \to z}\|_2^2 = \|T_{w \to z}\|_2^2 + \|T_{r \to z}\|_2^2 \tag{43}$$

As observed in Corollary 5.3, the optimal preview controller minimizes $\|T_{w \to z}\|_2$. Since X_{gg} and Y_g are the solutions to the DAREs associated with the problem of minimizing $\|T_{w \to z}\|_2$, we may use the results in Secs. 4.1 and 5.1 to write

$$\gamma_{wc}^2 = \mathrm{Tr}\{(D_{11gw} + D_{12} F_{0w})'(D_{11gw} + D_{12} F_{0w}) + (B_{1gw} + B_{2g} F_{0w})' X_{gg} (B_{1gw} + B_{2g} F_{0w})\}$$

$$\gamma_{wf}^2 = \mathrm{Tr}\{\bar{R}((L_{0y}\boldsymbol{D}_{21gw} - \boldsymbol{F}_{0w})(L_{0y}\boldsymbol{D}_{21gw} - \boldsymbol{F}_{0w})' + (L_{0y}\boldsymbol{C}_{2g} - \boldsymbol{F}_{2g})Y_{gg}(L_{0y}\boldsymbol{C}_{2g} - \boldsymbol{F}_{2g})')\}$$

$$\|T_{w\to z}\|_2^2 = \gamma_{wc}^2 + \gamma_{wf}^2$$

which are independent of the preview length.

We now turn our attention to the evaluation of $\|T_{r\to z}\|_2$. Since the signal r is "known" to the controller, it does not introduce an estimation error. As a result the output-feedback controller achieves exactly the same transfer function $T_{r\to z}$ as the full-information controller K_{FI}. Thus

$$T_{r\to z} = \left[\begin{array}{c|c} \boldsymbol{A} + \boldsymbol{B}_2\boldsymbol{F}_2 & \begin{bmatrix} \boldsymbol{B}_{2g}\boldsymbol{F}_{0r} \\ \boldsymbol{B}_p \end{bmatrix} \\ \hline \boldsymbol{C}_1 + \boldsymbol{D}_{12}\boldsymbol{F}_2 & \boldsymbol{D}_{12}\boldsymbol{F}_{0r} \end{array}\right]$$

Note that $\boldsymbol{X}$ satisfies

$$(\boldsymbol{A} + \boldsymbol{B}_2\boldsymbol{F}_2)'\boldsymbol{X}(\boldsymbol{A} + \boldsymbol{B}_2\boldsymbol{F}_2) + (\boldsymbol{C}_1 + \boldsymbol{D}_{12}\boldsymbol{F}_2)'(\boldsymbol{C}_1 + \boldsymbol{D}_{12}\boldsymbol{F}_2)$$

and so using Eq. (3) we may write

$$\|T_{r\to z}\|_2^2 = \mathrm{Tr}\left\{ (\boldsymbol{D}_{12}\boldsymbol{F}_{0r})'\boldsymbol{D}_{12}\boldsymbol{F}_{0r} + \begin{bmatrix} \boldsymbol{B}_{2g}\boldsymbol{F}_{0r} \\ \boldsymbol{B}_p \end{bmatrix}' \begin{bmatrix} X_{gg} & X_{gp} \\ X_{gp}' & X_{pp} \end{bmatrix} \times \begin{bmatrix} \boldsymbol{B}_{2g}\boldsymbol{F}_{0r} \\ \boldsymbol{B}_p \end{bmatrix} \right\}$$

where $\boldsymbol{F}_{0r} = -\bar{R}^{-1}\boldsymbol{B}_{2g}'\boldsymbol{X}_{gp}\boldsymbol{B}_p$. The above expression may be simplified to

$$\|T_{r\to z}\|_2^2 = \mathrm{Tr}\{\boldsymbol{B}_p'\boldsymbol{X}_{pp}\boldsymbol{B}_p - \boldsymbol{F}_{0r}'\bar{R}\boldsymbol{F}_{0r}\} \qquad (44)$$

Our next task is to find an efficient method for computing $\boldsymbol{B}_p'\boldsymbol{X}_{pp}\boldsymbol{B}_p$. Using the $W_r = I$ version of Eq. (17), we can write

$$\boldsymbol{X}_{pp} = \boldsymbol{A}_p'\boldsymbol{X}_{pp}\boldsymbol{A}_p + \hat{Q} - \boldsymbol{F}_{2p}'\bar{R}\boldsymbol{F}_{2p}$$

in which

$$\hat{Q} = \boldsymbol{C}_p'\boldsymbol{B}_{1gr}'\boldsymbol{X}_{gg}\boldsymbol{B}_{1gr}\boldsymbol{C}_p + \boldsymbol{A}_p'\boldsymbol{X}_{gp}'\boldsymbol{B}_{1gr}\boldsymbol{C}_p + \boldsymbol{C}_p'\boldsymbol{B}_{1gr}'\boldsymbol{X}_{gp}\boldsymbol{A}_p + \boldsymbol{C}_p'\boldsymbol{D}_{11gr}'\boldsymbol{D}_{11gr}\boldsymbol{C}_p$$

Substituting this into itself leads to

$$\boldsymbol{X}_{pp} = \sum_{j=0}^{N-1} \boldsymbol{A}_p^{j\prime}(\hat{Q} - \boldsymbol{F}_{2p}'\bar{R}\boldsymbol{F}_{2p})\boldsymbol{A}_p^j$$

Note that postmultiplying by $\boldsymbol{A}_p^k\boldsymbol{B}_p$ has the effect of selecting individual block columns of the preceding matrix that $\boldsymbol{C}_p\boldsymbol{A}_p^k\boldsymbol{B}_p = 0$, $\forall k \neq N-1$, and that $\boldsymbol{A}_p^N = 0$. This means that

$$\boldsymbol{B}_p'\boldsymbol{X}_{pp}\boldsymbol{B}_p = \boldsymbol{B}_{1gr}'\boldsymbol{X}_{gg}\boldsymbol{B}_{1gr} + \boldsymbol{D}_{11gr}'\boldsymbol{D}_{11gr} - \boldsymbol{F}_{2p0}'\bar{R}\boldsymbol{F}_{2p0} - \sum_{j=0}^{N-2} S'\boldsymbol{A}_{cg}^j\boldsymbol{B}_{2g}\bar{R}^{-1}\boldsymbol{B}_{2g}'\boldsymbol{A}_{cg}^j{}'S$$

where $\boldsymbol{F}_{2p0}$ is the leftmost block column of $\boldsymbol{F}_{2p}$ and is given by

$$\boldsymbol{F}_{2p0} = -\bar{R}^{-1}(\boldsymbol{B}_{2g}'\boldsymbol{X}_{gg}\boldsymbol{B}_{1gr} + \boldsymbol{D}_{12}'\boldsymbol{D}_{11gr}) \qquad (45)$$

Combining this with Eq. (44) and using Eq. (21), leads to

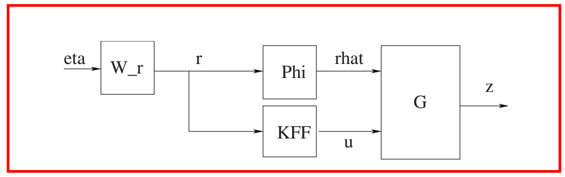

Fig. 6 A feedforward controller design problem. The notation follows that of Fig. 1.

$$\|T_{r\to z}\|_2^2 = \mathrm{Tr}\left\{ \underbrace{\boldsymbol{B}_{1gr}'\boldsymbol{X}_{gg}\boldsymbol{B}_{1gr} + \boldsymbol{D}_{11gr}'\boldsymbol{D}_{11gr} - \boldsymbol{F}_{2p0}'\bar{R}\boldsymbol{F}_{2p0}}_{\text{Zero preview}} - \underbrace{\sum_{j=0}^{N-1} S'\boldsymbol{A}_{cg}^j\boldsymbol{B}_{2g}\bar{R}^{-1}\boldsymbol{B}_{2g}'\boldsymbol{A}_{cg}^j{}'S}_{\text{Preview reduction}} \right\} \qquad (46)$$

In order to judge how much preview to use, we need to know the value of the maximum possible improvement due to preview action. Suppose the matrix $\boldsymbol{\Gamma}$ satisfies

$$\boldsymbol{\Gamma} = \boldsymbol{A}_{cg}\boldsymbol{\Gamma}\boldsymbol{A}_{cg}' + \boldsymbol{B}_{2g}\bar{R}^{-1}\boldsymbol{B}_{2g}'$$

By repeatedly substituting for $\boldsymbol{\Gamma}$ in the above equation, and noting that $\boldsymbol{A}_{cg}$ is stable, we can write

$$\boldsymbol{\Gamma} = \sum_{j=0}^{\infty} \boldsymbol{A}_{cg}^j\boldsymbol{B}_{2g}\bar{R}^{-1}\boldsymbol{B}_{2g}'\boldsymbol{A}'^j_{cg}$$

Comparing this to Eq. (46), it follows that the maximum reduction in $\|T_{r\to z}\|_2^2$ due to preview is given by

$$\mathrm{Tr}\{S'\boldsymbol{\Gamma}S\}$$

and evaluating this limit only requires the solution of an n_g-dimensional Lyapunov equation (in addition to the n_g-dimensional DARE required to evaluate S). The following quantity provides a useful measure of the fraction of the maximum norm reduction that has been achieved:

$$\gamma_{\%,imp} = 100 \times \mathrm{Tr}\left\{\left(\sum_{j=0}^{N-1} S'\boldsymbol{A}_{cg}^j\boldsymbol{B}_{2g}\bar{R}^{-1}\boldsymbol{B}_{2g}'\boldsymbol{A}_{cg}^j{}'S\right)\right\}/\mathrm{Tr}\{S'\boldsymbol{\Gamma}S\} \qquad (47)$$

This can be used to determine how much preview to use; for example, one might continue adding preview points until $\gamma_{\%,imp} > 95\%$.

7 Computation of a Preview Feedforward Controller

In this section we consider the problem of designing a feedforward controller. Such a problem may arise if there is no feedback signal, or if we wish to use a preview precompensator to enhance an existing feedback controller.

Potentially, one could formulate a feedforward problem by removing the measurement signal y from the configuration in Fig. 1. However, if we recall that

$$\|T_{[\eta' w']' \to z}\|_2^2 = \|T_{w\to z}\|_2^2 + \|T_{\eta\to z}\|_2^2$$

and that a feedforward controller does not alter $T_{w\to z}$, then it follows that $\|T_{[w'\,\eta']'\to z}\|_2$ is minimized by choosing the feedforward controller, which minimizes $\|T_{\eta\to z}\|_2$. Given these observations, we may neglect the influence of w in the design process.

The problem considered in this section is illustrated in Fig. 6. Such a configuration is apparently a special case of Fig. 1, and so it is tempting to try to tackle this problem by using the above general theory with y set to zero (by setting $\boldsymbol{D}_{21gw}$, $\boldsymbol{D}_{21gr}$, $\boldsymbol{C}_{2g}$, and

D_{22g} to zero) and with w removed. Unfortunately, such an approach does not succeed because assumption (A5) is violated. We will now derive a solution to this problem.

By modifying Eq. (4), it follows that the appropriate generalized plant is given by

$$P_{FI} \stackrel{s}{=} \begin{bmatrix} A_g & B_{1gr}C_{d1} & 0 & B_{2g} \\ 0 & A_d & B_d & 0 \\ C_{1g} & D_{11gr}C_{d1} & 0 & D_{12} \\ 0 & C_{d2} & D_r & 0 \end{bmatrix} \tag{48}$$

$$= \begin{bmatrix} A & B_1 & B_2 \\ C_1 & D_{11} & D_{12} \\ C_2 & D_{21} & 0 \end{bmatrix} \tag{49}$$

It is easily checked that the associated full-information control is obtained by removing the gain associated with w, and so $K_{FI} = [F_{2g}\ F_{2p}\ F_{2r}\ F_{0r}]$, where the gains may be computed using Eqs. (14) and (26)–(28). To arrive at this result, one only needs to retrace the derivations of Sec. 4, with B_{1gw} and D_{11gw} set to zero.

Next, we give a result concerning the solution to the estimation DARE.

Lemma 7.1. *If A_g is stable and W_r is outer, then the version of the DARE in Eq. (32) associated with Eq. (48) has a stabilizing solution $Y=0$.*

Proof. First, note that if $Y=0$, then

$$L_2 = -\begin{bmatrix} 0 \\ B_d D_r^{-1} \end{bmatrix}$$

$$\bar{S} = D_r D_r'$$

from which it can be checked that $Y=0$ solves Eq. (32). This solution is stabilizing because

$$A + L_2 C_2 = \begin{bmatrix} A_g & B_{1gr}C_{d1} \\ 0 & A_d - B_d D_r^{-1} C_{d2} \end{bmatrix}$$

is stable since A_g is stable and W_r is outer (see Eq. (40)).

If we also note that

$$L_0 = F_{0r} D_r^{-1}$$

with F_{0r} defined in Eq. (28), then we can use Eq. (33) to obtain the following $\mathcal{H}_2$-optimal controller

$$K_{FI} \stackrel{s}{=} \begin{bmatrix} A_K & B_K \\ C_K & D_K \end{bmatrix}$$

$$A_K = \begin{bmatrix} A_g + B_{2g}F_{2g} & B_{1gr}C_p + B_{2g}F_{2p} & B_{2g}F_{2r} - B_{2g}F_{0r}D_r^{-1}C_r \\ 0 & A_p & 0 \\ 0 & 0 & A_r - B_r D_r^{-1} C_r \end{bmatrix}$$

$$B_K = \begin{bmatrix} B_{2g}F_{0r}D_r^{-1} \\ B_p \\ B_r D_r^{-1} \end{bmatrix}$$

$$C_K = \begin{bmatrix} F_{2g} & F_{2p} & F_{2r} - F_{0r}D_r^{-1}C_r \end{bmatrix}$$

$$D_K = F_{0r} D_r^{-1}$$

which has the low-order representation

Pretty hard to follow the flow of the columns on this page.

$$\bar{K}_{FF} \stackrel{s}{=} \begin{bmatrix} A_g + B_{2g}F_{2g} & B_{2g}F_{2r} - B_{2g}F_{0r}D_r^{-1}C_r & B_{1gr}C_p + B_{2g}F_{2p} & B_{2g}F_{0r}D_r^{-1} \\ 0 & A_r - B_r D_r^{-1} C_r & 0 & B_r D_r^{-1} \\ F_{2g} & F_{2r} - F_{0r}D_r^{-1}C_r & F_{2p} & F_{0r}D_r^{-1} \end{bmatrix}$$

such that the optimal control is given by

$$u^* = \bar{K}_{FF}\bar{r}$$

in which

$$\bar{r}(k) = \begin{bmatrix} r(k-N) \\ \vdots \\ r(k) \end{bmatrix}$$

8 Summary of Results

Our purpose here is to provide a summary of the major features of $\mathcal{H}_2$ preview controllers, which will hopefully be of assistance to control system designers. While some of these results are known within the control systems community, they are spread over many publications spanning three decades.

8.1 Generic Controller Features

Insert "equation"

8.1.1 Riccati Equation Solutions. Synthesizing the output-feedback controller requires the solution of a full-information Riccati equation and a Kalman filtering [16,17]. Although these equations appear to be of high order, the full-information control problem only requires the solution of the n_g-dimensional Riccati equation (13), while the estimation problem requires the solution of the n_g-dimensional Riccati equation (38). The bulk of the full-information Riccati equation can be evaluated using the linear equations (16) and (17). The DARE in Eq. (13) is precisely that which would be obtained if one were to search for a full-information controller, which minimized $\|T_{w\to z}\|$.

It is important to note that F_{2g} and $\bar{R}$ are not functions of X_{gd} or X_{dd}, and so Eq. (13) may be solved independently of Eqs. (16) and (17). However, Eq. (16) depends on the solution of Eq. (13), and Eq. (17) depends on both Eqs. (13) and (16). Lemma 4.2 provides a fast algorithm for solving Eq. (16).

8.1.2 Full-Information Control Structure. The full-information control signal has the form

$$u(k)^* = \hat{u}(k) + \sum_{j=0}^{N-1} F_{2p,j} r(k-N+j)$$

in which $\hat{u}(k)$ is a linear function of the states of G and W_r, and of the signals η and w; the $F_{2p,j}$ are sometimes referred to as the "preview gains." Further insight into the structure and role of the control signal components can be found in Remarks 4.5–4.7.

8.1.3 The Preview Gains Decay to Zero as $N\to\infty$. It was first noted in Ref. [6] that the magnitude of the preview gains approaches zero as N approaches infinity; this follows from Eq. (26) and $\lim_{N\to\infty} A_{cg}^N = 0$. As a consequence, far-distant preview information is relatively less important and the optimal infinite preview controller can be approximated to arbitrary accuracy using a finite preview length.

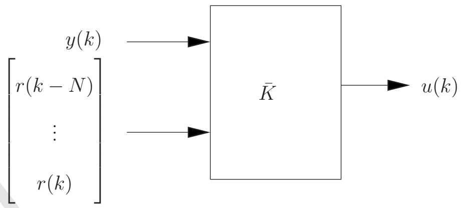

Fig. 7 The structure of the $\mathcal{H}_2$-optimal discrete-time preview controller. The signal $u(k)$ is the control, the measurement is $y(k)$, and $r(k)$ is the futuremost value of the previewable disturbance.

8.1.4 The Controller Has FIR (Preview) and IIR Components. Discrete-time preview controllers are composed of a high-order FIR preview component and low-order IIR components. This structure is illustrated in Fig. 5, and is also highlighted in the continuous-time case in Ref. [22]. A proof is provided for the discrete-time case in Sec. 5. If the controller is written in observer form, then the states of the FIR preview block and the order n_r IIR block are (perfect) reconstructions of the states of Φ and W_r, respectively. The state of the order n_g IIR block is an estimate for the state of G.

8.1.5 The Controller is Essentially Low-Order. A discrete-time FIR transfer function can be realized using a shift-register to update the state, and a gain array to compute the output. This representation leads to the low-order controller representation in Fig. 7, where $\bar{K}$ is given by Eq. (42).

8.1.6 The Optimal Control is Independent of W_r for Large N. This phenomenon was first noticed in Ref. [6], with a proof provided in Sec. 4. It is instructive to consider the influence of W_r from a stochastic perspective. Since η is assumed to be a realization of a white-noise process, then a dynamic W_r provides statistical information on future values of r. If, for example, W_r is low-pass, the $r(k)$ becomes correlated and hence W_r introduces "statistical preview" beyond the preview horizon. We would therefore expect W_r to reduce the need for preview, and also that its influence on the control would decline as N tends to infinity.

8.1.7 The Optimal $\|T_{w\to z}\|_2$ Is Independent of W_r. In contrast with the $\mathcal{H}_\infty$ case [23], there is no conflict between the rejection of w and the rejection of η; a proof of this is provided in Sec. 5.

8.1.8 Noisy Preview Signals Require a High-Order Controller. One might consider an uncertain preview problem, where the controller has access only to a noise-corrupted version of the previewed signal. In this scenario, the states of Φ are not known, and must be estimated. The preview provides benefit both by reducing the full-information control cost and by reducing the estimation cost. Estimating the states of Φ is a type of fixed-lag smoothing problem. Low-order implementations of fixed-lag smoothers are given in Ref. [24], but these implementations are not usable here because of the need for an estimate of all of the states of Φ, rather than just the output of Φ. The resulting controller is thus of the same order as the augmented plant. A controller for this problem may be synthesized by direct application of the results in Sec. 5.1.

8.2 Design Insights. This section provides a number of "rules of thumb" that the authors have found useful. For the purposes of illustration, we will consider the full-information preview-tracking problem described in Fig. 8, where G is given by

$$\hat{G} = \frac{1.26\times 10^{-8}(\mathcal{Z}+1)^3}{(\mathcal{Z}-1)(\mathcal{Z}^2-1.998\mathcal{Z}+0.998)}$$

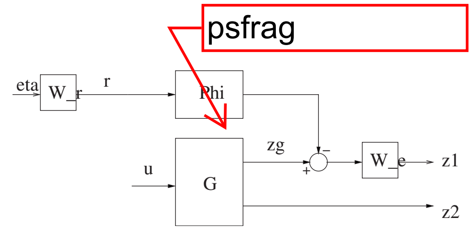

Fig. 8 A simple preview-tracking problem. The feedback signal is derived from the states of G, W_r, W_e, and Φ, together with η. The signal u is the control, r is the previewed reference, and $z=[z_1' z_2']'$ is the output to be minimized.

$$G = \begin{bmatrix} \hat{G} \\ 1 \end{bmatrix} \qquad (50)$$

The discrete transfer function $\hat{G}$ was obtained by discretizing

$$\frac{101}{s(s^2+2s+101)}$$

using a sample time of 0.001 s. We search for a K that minimizes $\|T_{\eta\to z}\|_{2,\infty}$, or equivalently, the K that minimizes

$$\left\| \begin{bmatrix} W_e W_r T_{r\to e} \\ W_r T_{r\to u} \end{bmatrix} \right\|_{2,\infty} \qquad (51)$$

Clearly, this represents a tracking problem in which minimization of tracking errors must be balanced against excessive control requirements. The transfer functions W_r and W_e may be chosen to reflect, respectively, the expected frequency content of r, and the importance of achieving good tracking at a given frequency. We will now use this example to illustrate some general properties of $\mathcal{H}_2$ preview-tracking controllers.

8.2.1 Preview Improves Steady-State Tracking. Figure 9 illustrates the "nonresponsiveness" of the closed-loop system in the case of no reference weight and a low preview horizon. In the limiting case, where there is zero preview and no reference weighting, the controller does not have any information about the value of the reference at the next time step, and so it cannot make a decision about the direction in which to send the plant. Therefore, the tracking-error cost cannot be reduced, and so the optimal controller can only minimize the control cost, leading to a choice of $u=0$.

Alternatively, as $N\to\infty$, then the steady-state error tends toward zero (in the absence of disturbances or modeling errors).

8.2.2 Reference Weighting Introduces Stochastic Preview. The responses illustrated in Fig. 9 are unsatisfactory for preview horizons of less than $N=200$. When short preview horizons are mandated, a low-pass W_r improves low-frequency tracking by biasing the controller optimization toward lower frequencies. It is worth noting, however, that care should be taken in choosing W_r. If, for example, W_r rolls off too quickly, the closed-loop will be poorly tuned for step inputs and can have an oscillatory response, and/or high-amplitude controls. This is because a low-pass W_r has the dual effect of penalizing low-frequency tracking errors, and also reducing the penalty on high frequency controls—see Eq. (51). The effect of a low-pass W_r is illustrated in Fig. 10.

8.2.3 Tracking-Error Filtering. Consider the full-information controller synthesis problem illustrated in Fig. 8 and let W_e be a dynamic tracking-error filter. A low-pass weight on the tracking error improves the low-frequency tracking performance, without needing to change the assumed frequency content of the reference signal (i.e., without changing W_r). Note that a step change in the reference does not lead to a "spike" in the control signal—see Fig. 12.

8.2.4 Improving the Low-Frequency Tracking Behavior. It appears that there are three alternative ways of improving the low-

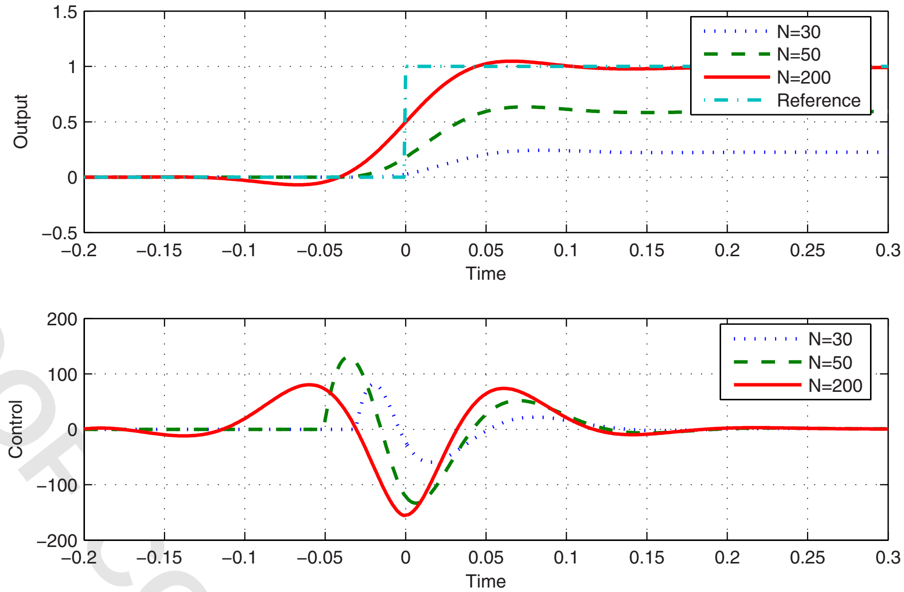

Fig. 9 Closed-loop response of the system described in Eq. (50) and Fig. 8 with W_r=1 and W_e=1000. The plotted output is the signal z_g in Fig. 8, and shows the relative nonresponsiveness of the low-preview-horizon system.

frequency tracking behavior, which could be used alone or in combination: (a) use a long preview horizon, (b) add a low-pass reference filter, and (c) introduce a low-pass tracking-error filter. These alternatives are illustrated in Fig. 11. In order to achieve a fair comparison, W_e was scaled so that the resulting closed loops achieved approximately similar rise times. The tracking-error filter achieves good steady-state performance without excessive control or large control spikes. However, the introduction of a tracking-error filter tends to introduce additional phase lag, which can have a deleterious effect on the loop's robust stability. In contrast, the feedback part of the controller is independent of W_r, which means that a reference filter can be used without jeopardizing stability.

8.2.5 Preview Reduces the Peak Control Magnitude. Figure 12 illustrates the influence of preview on the control magnitude. In this example, the output response is not strongly influenced by changes in the preview horizon, but the peak control magnitude reduces substantially as the preview horizon increases. This effect can be very useful in application in which control ceilings are a limiting factor, and one wishes to maintain a short rise time.

8.2.6 Preview Only Improves Low-Frequency Tracking Performance. For a low-pass plant, high frequency tracking performance is limited by the prohibitive amplitude of the control action. This is a fundamental feature of the plant and cannot be changed by anticipative action. This effect is illustrated in Figs.

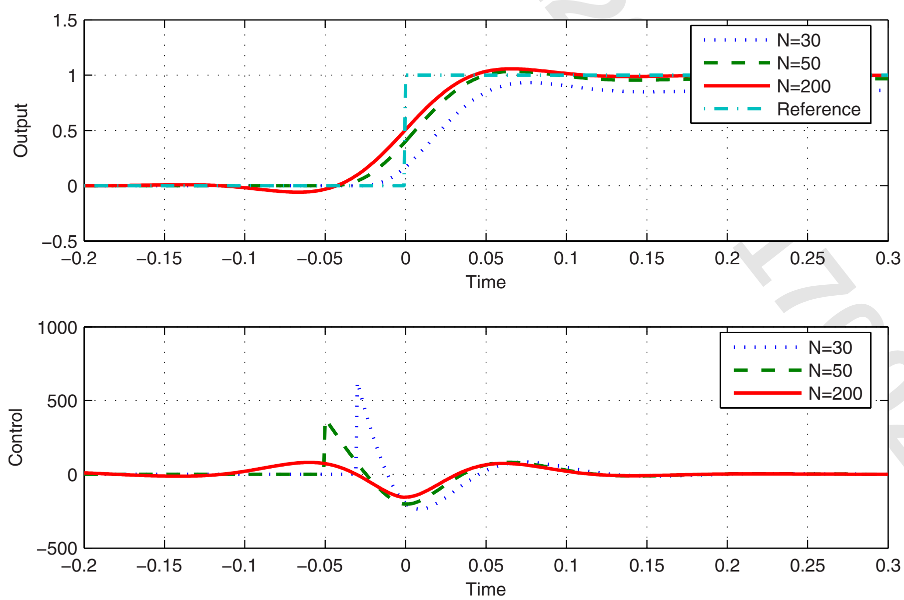

Fig. 10 Closed-loop response of the system described in Eq. (50) and Fig. 8; the reference weight is given by $W_r = \mathcal{Z}/(\mathcal{Z}-0.99)$, with W_e=1000. The improved step response (of z_g) for short preview horizons is clearly visible. Note the high-amplitude control in the N=30 case.

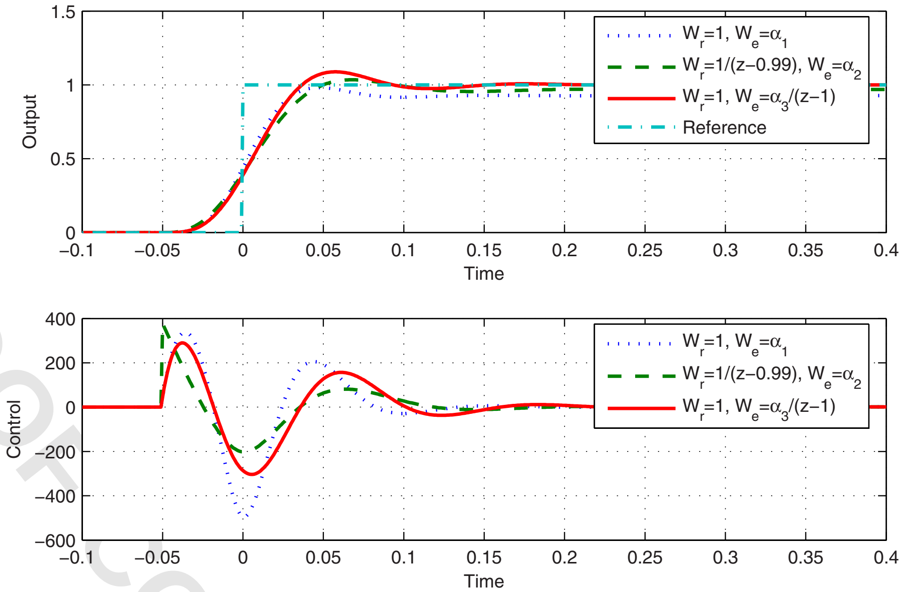

Fig. 11 Closed-loop response of the example system described in Eq. (50) and Fig. 8. The preview horizon is fixed at $N=50$ and α_i is used to achieve similar closed-loop rise times. While the closed-loop responses (z_g) are similar, the control signals are quite different; especially near the beginning of the preview horizon.

13(*a*) and 13(*b*), where preview improves the low-frequency performance by reducing the magnitude of both the tracking error and the control signal.

8.2.7 Integral Action With Output Feedback. An output-feedback tracking controller with integral action is described by Fig. 14, which also serves to illustrate the complexity of problems that may be tackled using the framework in Fig. 1. Note that the integrated error signal must be included in the measurements in order to ensure that the integrator state is detectable.

Tuning the relative magnitudes of W_{e1} and W_{e2} is akin to adjusting the gains in a PI controller. In fact a derivative signal could also be added, thus completing the PID analogy and facilitating tuning of the preview controller.

Previously, the addition of integral action has been approached in a LQG setting through the use of the differentiated control signal in the cost function (e.g., Refs. [7,25,8]). Such an approach does not allow one to adjust the strength of the integral action, which is likely to lead to difficulty in satisfying stability/performance requirements.

9 Concluding Remarks

Preview control has been studied for at least four decades and a large number of theoretical results can be found in the control and mechanical engineering technical literature. In many cases the

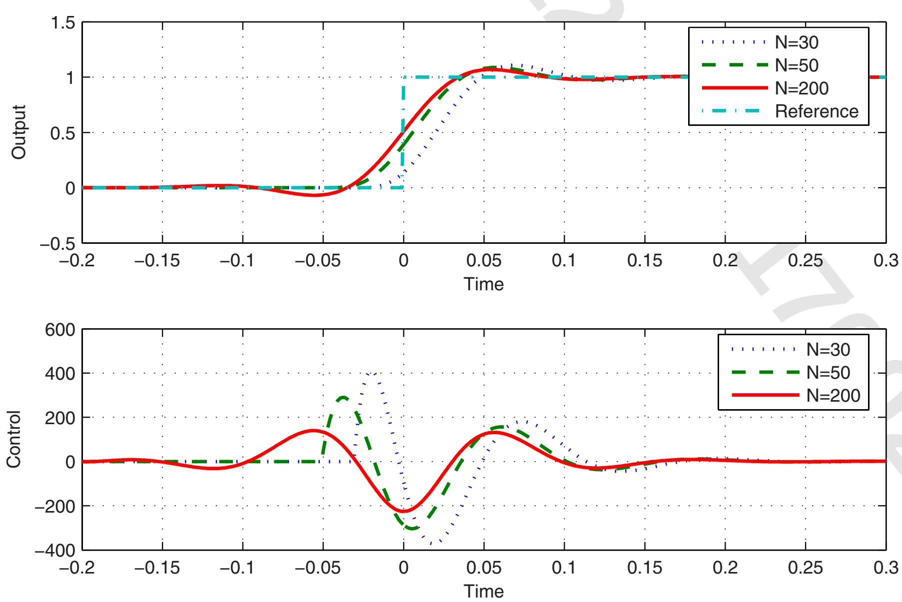

Fig. 12 Closed-loop response of the example system described in Eq. (50) and Fig. 9; the weighting functions are $W_r=1$ and $W_e=100/(1-\mathcal{Z})$. The plotted output is the signal z_g in Fig. 8, and is relatively insensitive to the preview horizon. The control signal becomes "spread out," and lower in amplitude, as the preview horizon is increased.

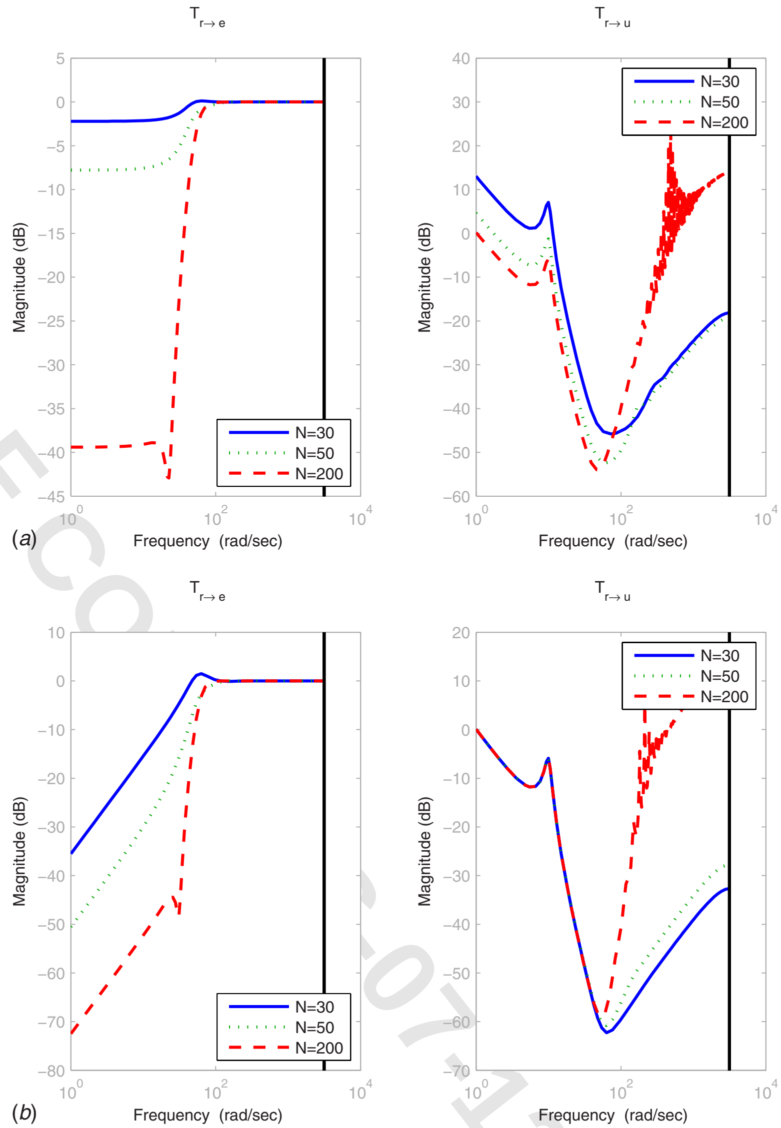

Fig. 13 Bode plots of the closed-loop transfer functions $T_{r\to e}$ and $T_{r\to u}$, which result from the application of the $\mathcal{H}_\infty$-optimal controls. The unweighted plant is considered in (*a*), and a low-pass W_e ($W_e=1/(\mathcal{Z}-1)$) is employed in (*b*).

"can be found in the author's thesis, Ref [21]"

theoretical developments on discrete-time $\mathcal{H}_2$/LQG were driven by applications problems. Contemporary applications include for example active automotive suspension control [14,13], helicopter

psfrag

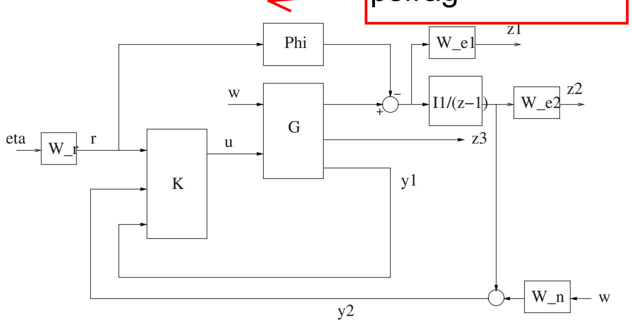

Fig. 14 Preview tracking with integral action. The signal $z=[z_1' z_2' z_3']'$ is the output of the closed-loop transfer function whose $\mathcal{H}_2$-norm is to be minimized; $y=[y_1' y_2']'$ is the measurement signal. The transfer functions W_{e1}, W_{e2}, and W_n are shaping filters. The other notation follows that of Fig. 1.

flight control [26], and driver steering control [27]. Other applications examples, which are also related to vehicle dynamics problems, can be found in the thesis done by author Hazell.[2] A MATLAB preview control toolbox implementing the presented algorithms, together with th is also available [footnote 2]. ~~be obtained from this site.~~

In the authors' opinion, the strong influence of applications problems has produced a body of theory that is example-specific and consequently somewhat restricted in terms of its scope and generality. To the best of their knowledge, a complete set of tools for synthesizing $\mathcal{H}_2$ preview controllers that solve a broad range of realistic design problems is unavailable in the open literature. The provision of these tools is the central purpose of the work presented here. The authors present a general preview problem that captures most of the results in the contemporary literature, as well as offering a solution framework for more complex preview problems such as the preview tracking with integral action problem illustrated in Fig. 14.

[2]http://code.google.com/p/preview-control-toolbox/.

The preview control problem studied in this paper is shown in Fig. 1, and it comprises a plant that is controlled by a two-degrees-of-freedom controller. The controller is synthesized to optimize the closed-loop system's response to a combination of previewable and nonpreviewable exogenous inputs. The presented solution includes an efficient computational framework that is based on two low-order Riccati equations with dimension that of the plant (excluding the preview delay line). This algorithm also includes an efficient computation of the perfect information controller gains as well as the controller itself. We have also provided an efficient method for finding the $\mathcal{H}_2$-norm of the closed-loop system, and a method for evaluating the norm reduction due to preview as $N \rightarrow \infty$. As is shown in Figs. 4 and 7, the controller structure is essentially low-order with the preview part implemented using an efficient finite-impulse-response section.

Acknowledgment

This work was supported by a portfolio partnership held with the British Engineering and Physical Sciences Research Council (EPSRC), and also by the Flapless Air Vehicle Integrated Industrial Research program funded by BAe Systems and the EPSRC.

References

[1] Sheridan, T. B., 1966, "Three Models of Preview Control," IEEE Trans on Human Factors in Electronics, **HFE-7**(2), pp. 91–102.

[2] Bender, E. K., 1968, "Optimal Linear Preview Control With Application to Vehicle Suspension," Trans. ASME, **90**(2), pp. 213–221.

[3] Tomizuka, M., 1973, "The Optimal Finite Preview Problem and Its Application to Man-Machine Systems," Ph.D. thesis, Massachusetts Institute of Technology, Cambridge, MA.

[4] Tomizuka, M., 1975, "Optimal Continuous Finite Preview Problem," IEEE Trans. Autom. Control, **20**(3), pp. 362–365.

[5] Lindquist, A., 1968, "On Optimal Stochastic Control With Smoothed Information," Inf. Sci. (N.Y.), **1**(1), pp. 55–85.

[6] Tomizuka, M., and Whitney, D. E., 1975, "Optimal Discrete Finite Preview Problems (Why and How Is Future Information Important?)," ASME J. Dyn. Syst., Meas., Control, **97**(4), pp. 319–325.

[7] Tomizuka, M., and Rosenthal, D. E., 1979, "On the Optimal Digital State Vector Feedback Controller With Integral and Preview Actions," ASME J. Dyn. Syst., Meas., Control, **101**(2), pp. 172–178.

[8] Tomizuka, M., and Fung, D., 1980, "Design of Digital Feedfoward/Preview Controllers for Processes With Predetermined Feedback Controllers," ASME J. Dyn. Syst., Meas., Control, **102**(4), pp. 218–225.

[9] Zattoni, E., 2006, "$\mathcal{H}_2$-Optimal Decoupling With Preview: A Dynamic Feedforward Solution Based on Factorization Techniques," Proceedings of the 2006 American Control Conference, IEEE, pp. 316–320.

[10] Marro, G., and Zattoni, E., 2005, "$\mathcal{H}_2$-Optimal Rejection With Preview in the Continuous-Time Domain," Automatica, **41**(5), pp. 815–821.

[11] Tomizuka, M., 1976, "Optimal Preview Control With Application to Vehicle Suspension—Revisited," ASME J. Dyn. Syst., Meas., Control, **98**(3), pp. 362–365.

[12] Hac, A., 1992, "Optimal Linear Preview Control of Active Vehicle Suspension," Veh. Syst. Dyn., **21**(1), pp. 167–195.

[13] Marzbanrad, J., Ahmadi, G., Zohoor, H., and Hojjat, Y., 2004, "Stochastic Optimal Preview Control of a Vehicle Suspension," J. Sound Vib., **275**(3–5), pp. 973–990.

[14] Roh, H. S., and Park, Y., 1999, "Stochastic Optimal Preview Control of an Active Vehicle Suspension," J. Sound Vib., **220**(2), pp. 313–330.

[15] Sharp, R. S., 2005, "Driver Steering Control and a New Perspective on Car Handling Qualities," Proc. Inst. Mech. Eng., Part C: J. Mech. Eng. Sci., **219**(10), pp. 1041–1051.

[16] Green, M., and Limebeer, D. J. N., 1995, *Linear Robust Control*, Prentice-Hall, Englewood Cliffs, NJ.

[17] Zhou, K., Doyle, J., and Glover, K., 1996, *Robust and Optimal Control*, Prentice-Hall, Englewood Cliffs, NJ.

[18] Doyle, J. C., Francis, B. A., and Tannenbaum, A. R., 1990, *Feedback Control Theory*, Macmillan, New York.

[19] Middleton, R. H., Chen, J., and Freudenberg, J. S., 2004, "Tracking Sensitivity and Achievable $\mathcal{H}_\infty$ Performance in Preview Control," Automatica, **40**(8), pp. 1297–1306.

[20] Houpis, C. H., and Lamont, G. B., 1991, *Digital Control Systems*, 2nd ed., McGraw-Hill, New York.

[21] Hazell, A. J., 2008, "Discrete-Time Optimal Preview Control," Ph.D. thesis, Imperial College, London, http://deposit.depot.edina.ac.uk/145/

[22] Moelja, A. A., and Meinsma, G., 2006, "$\mathcal{H}_2$ Control of Preview Systems," Automatica, **42**(6), pp. 945–952.

[23] Hazell, A. J., and Limebeer, D. J. N., 2008, "An Efficient Algorithm for Discrete-Time $\mathcal{H}_\infty$ Preview Control," Automatica, **44**(9), pp. 2441–2448.

[24] Anderson, B. D. O., and Moore, J. B., 1979, *Optimal Filtering*, Prentice-Hall, Englewood Cliffs, NJ.

[25] Katayama, T., and Hirono, T., 1987, "Design of an Optimal Servomechanism With Preview Action and Its Dual Problem," Int. J. Control, **45**, pp. 407–420.

[26] Paulino, N., Cunha, R., and Silvestre, C., 2006, "Affine Parameter-Dependent Preview Control for Rotorcraft Terrain Following Flight," J. Guid. Control Dyn., **29**(6), pp. 1350–1359.

[27] Cole, D. J., Pick, A. J., and Odhams, A. M. C., 2006, "Predictive and Linear Quadratic Methods for Potential Application to Modelling Driver Steering Control," Veh. Syst. Dyn., **44**(3), pp. 259–284.

PROOF COPY [DS-07-1223] 017002JDS

NOT FOR PRINT! FOR REVIEW BY AUTHOR NOT FOR PRINT!

AUTHOR QUERIES — 017002JDS

Linear Quadratic

#1 AU: Please provide the definitions of LQ and other undefined acronyms in this document, if possible.

#2 AU: Please verify changes made from "Bender's vehicle suspension preview problem is re-visited in (11)" to "The vehicle suspension preview problem by Bender [2] is revisited in Ref. [11]" and check if intended meaning is preserved.

OK

#3 AU: Please verify that the volume should be "HFE-7" not "7" in Ref. 1.

OK

#4 Author: Please supply full journal title, the CODEN, and/or ISSN for journal in Ref. 2.

Bender, E. K., Optimal linear preview control with
application to vehicle suspension, ASME Journal of Basic
Engineering, Ser. D, Vol. 90, No. 2, pp. 213-221, 1968

#5 AU: Please verify changes made in the issue numbers of Refs. 12 and 13.

Correct

#6 AU: Please note and verify all changes made to the figure captions of 017002jds.

can't see any changes (assuming this is fig 1 or 3)